

Phase Identifications in Crud from Commercial Boiling Water Reactors at the Idaho National Laboratory by Transmission Electron Microscopy

**2007 International LWR Fuel
Performance Meeting**

Dawn E. Janney
Douglas L. Porter
Joshua L. Peterson

September 2007

The INL is a
U.S. Department of Energy
National Laboratory
operated by
Battelle Energy Alliance



This is a preprint of a paper intended for publication in a journal or proceedings. Since changes may be made before publication, this preprint should not be cited or reproduced without permission of the author. This document was prepared as an account of work sponsored by an agency of the United States Government. Neither the United States Government nor any agency thereof, or any of their employees, makes any warranty, expressed or implied, or assumes any legal liability or responsibility for any third party's use, or the results of such use, of any information, apparatus, product or process disclosed in this report, or represents that its use by such third party would not infringe privately owned rights. The views expressed in this paper are not necessarily those of the United States Government or the sponsoring agency.

Phase Identifications in Crud from Commercial Boiling Water Reactors at the Idaho National Laboratory by Transmission Electron Microscopy

Dawn E. Janney and Douglas L. Porter
Center for Nuclear Fuels and Materials Research
Idaho National Laboratory

P.O. Box 1625, Idaho Falls, ID 83415-6188
Tel: 208-533-7478, Fax: 208-533-7996, Email: dawn.janney@inl.gov

Joshua L. Peterson
The University of Texas at Austin
Austin, TX 78758

Abstract – This paper reports results of research in which transmission electron microscopy was used to characterize phases in four samples of “crud” (activated corrosion products) from three commercially operating boiling water reactors. Samples A (from Reactor A) and B (from Reactor B) were collected by scraping crud deposits formed on the outsides of fuel pins in a hot cell. Both pins had thick deposits of tenacious crud. Samples C and D (both from Reactor C) were collected by sucking pool water through filters after brushing or scraping fuel pins in the pool. Sample A contained nanocrystalline areas and single euhedral crystals of franklinite (ZnFe_2O_4 , also known as zinc ferrite), single crystals of hematite ($\alpha\text{-Fe}_2\text{O}_3$), a nanocrystalline iron-oxide mixture that also probably includes goethite ($\alpha\text{-FeOOH}$) and magnetite (Fe_3O_4) or maghemite ($\gamma\text{-Fe}_2\text{O}_3$) but does not include significant quantities of akaganéite ($\beta\text{-FeOOH}$) or lepidocrocite ($\gamma\text{-FeOOH}$), crystalline silica (probably quartz, $\alpha\text{-SiO}_2$), and an unidentified high-Ba, high-S phase. Sample B contained euhedral crystals of franklinite, a single crystal of willemite (Zn_2SiO_4), several areas of nanocrystalline akaganéite ($\beta\text{-FeOOH}$), amorphous silica, and an unidentified Fe-Cr phase with significant concentrations of Ni and Si. Samples A and B contained halite (NaCl), and Sample A contained small quantities of sylvite (KCl). Sample C contained hematite, probably magnetite, at least one kind of clay, and a high-Pb particle. Several particles from Sample C have thick, high-Zr central parts surrounded by thin areas consisting of Fe oxides (primarily hematite); these particles may represent fragments of the cladding and immediately adjacent crud. Phases identified in Sample D include corundum ($\alpha\text{-Al}_2\text{O}_3$), hematite, an unidentified aluminosilicate that is probably a clay, and a high-Zr phase that was not analyzed in detail but may be part of the cladding.

Because significant concentrations of chloride would not be tolerated in reactor cooling systems, the halite and sylvite in Samples A and B are assumed to represent contaminants. Despite its nominal composition, akaganéite is a chloride-bearing phase, and also indicates contamination of Sample B. Corundum and clays are also likely contaminants. The presence of contaminants such as these must be considered in interpreting bulk chemical analyses.

Data from transmission electron microscopy provides detailed information about the microstructures, crystal structures, and compositions of a small number of tiny areas. Although this information cannot be obtained using other techniques, it should not be considered statistically representative and must be interpreted in the context of data representing larger volumes of material.

I. INTRODUCTION

Activated corrosion products (“crud”) from boiling-water reactors deposit primarily on the outer surfaces of fuel rods,¹ where they can lead to fuel-rod failures and cladding breaches. Crud can also become detached in cooling water and storage systems,² causing additional radiation exposure to plant workers. Despite its importance, crud is difficult to characterize by direct analysis, and there are few characterization papers in the open literature. Previous approaches to understanding crud

formation include studying corrosion products formed in boiling water with a composition similar to that in reactor cooling systems,^{3,4} predicting minerals expected to form based on models of the effects of radiolysis of water,⁵ and attempting to infer the phases present from analyses of samples involving large numbers of crystals.

Although each of these approaches provides important information, none of them directly identifies the crystal structures and compositions of individual phases present in

crud from operating reactors. To address this need, four samples of crud from three commercial boiling water reactors (BWRs) were analyzed at the Idaho National Laboratory. The results of these analyses were published in more detail elsewhere.^{6,7}

II. SAMPLES AND METHODS

As part of a continuing effort to improve the Department of Energy's ability to address problems in currently operating commercial nuclear reactors, the Electric Power Research Institute (EPRI) arranged for the Idaho National Laboratory (INL) to be sent four samples of crud from three commercial BWRs for analysis. Samples A and B (from Reactors A and B, respectively) were reported to be collected by scraping them from the outsides of fuel pins taken from the reactors during normal refueling operations. Sample A was collected at the 90-inch (~229 cm) elevation of a failed two-cycle rod that had a cumulative burnup of 38.3 GWd/MTU. Sample B was collected from the 30-inch (~76 cm) elevation on a sound three-cycle rod that had a cumulative burnup of 40.7 GWd/MTU. Both rods had thick deposits of tenacious crud, and both samples were from plants that used Zn addition and Noble Metal Chemical Addition (NMCA). Samples C and D (both from reactor C) were collected by sucking pool water through a filter after scraping and/or brushing the outside of the fuel pins in the pool. Sample C is from the ~45 cm (~17.7 inch) elevation of a sound one-cycle bundle with 21.9 GWd/MTU burnup, and Sample D is from the ~254 cm (~100 inch) level of a sound 1-cycle bundle with 22.2 GWd/MTU burnup.

Small particles from each of the four samples were prepared by placing a small particle or piece of filter paper in de-ionized water and ultrasonicated. A drop of water with suspended particles was deposited on a commercially prepared carbon-coated formvar substrate supported by a gold grid and air dried. A number of individual particles from each sample were analyzed using a JEOL 2010 transmission electron microscope (TEM) with a LaB6 filament operating at a nominal voltage of 200 kV. Images and diffraction patterns were collected with a Gatan Ultrascan camera and Gatan Digital Micrograph software, version 3.10.0 for GMS 1.5.0. Camera constants relating distances measured on diffraction patterns to lattice-plane spacings ("d-spacings") were calibrated using diffraction patterns from nanocrystalline gold. Energy-dispersive x-ray spectra (EDX) were collected with an Oxford Link Petafet EDX detector with a SiLi crystal, nominal 20 eV channel width, nominal energy range from 0 to 20 keV, and nominal 136 eV resolution. The spectra were collected and quantified using Link ISIS software, Isis Suite revision 3.2, with peak profiles and k-factors supplied by the manufacturer. Peaks from Au were assumed to be artifacts introduced by the grid, and only peaks representing elements with atomic numbers greater than 10 (i.e., Na and

higher) were considered in quantification. Individual phases were identified by comparing chemical and diffraction data to materials in the PDF4+ database (International Centre for Diffraction Data) and to publications in the mineralogical and crystallographic literature.

Samples, analytical methods, and results are described in more detail elsewhere.^{6,7}

III. RESULTS

Halite (NaCl) was identified in Samples A and B, and sylvite (KCl) was identified in Sample B. As it is highly unlikely that significant concentrations of chloride would be tolerated in a reactor cooling system, a sample of water from the wash bottle used for TEM sample preparation was analyzed for chloride concentration to determine whether the chloride needed to form these phases might have been accidentally introduced during sample preparation. Ion chromatography showed that the water had 0.3-0.4 ppm chloride—somewhat higher than would be expected from ultrapure water, but clearly not enough to be the source of the chlorine in the observed chlorides. Although the source of the chlorine remains unknown, it apparently represents a contaminant introduced between the time the fuel pins were removed from the reactor and the time the samples were sent to the INL for analysis. Because the halite and sylvite are contaminants, they will not be considered further in this paper.

III.A. Sample A

Franklinite (ZnFe_2O_4 , also known as zinc ferrite) occurred as nanocrystalline materials and euhedral single crystals in Sample A (Fig. 1). In addition to Zn and Fe, EDX spectra from franklinite in Sample A show small concentrations of Cr, Al, Mn, and Ni. As these elements can occur in solid solutions in franklinite⁸ and in separate crystals whose structure and lattice parameters are sufficiently similar to those of franklinite that they would probably not be detected in franklinite diffraction patterns,^{9,10} it was not possible to identify the host phases for these elements.

The most commonly observed iron oxide in Sample A was hematite, $\alpha\text{-Fe}_2\text{O}_3$, which occurred both as single crystals and in mixtures with other iron oxides (Fig. 2). D-spacings of rings in diffraction patterns from these mixtures were consistent with the presence of goethite ($\alpha\text{-FeOOH}$) and magnetite (Fe_3O_4) or maghemite ($\gamma\text{-Fe}_2\text{O}_3$) in addition to the hematite, but not with significant numbers of randomly oriented crystallites of akaganéite ($\beta\text{-FeOOH}$) or lepidocrocite ($\gamma\text{-FeOOH}$).

Other phases identified in Sample A include crystalline silica (probably quartz, $\alpha\text{-SiO}_2$), and a high-Ba, high-S phase that could not be identified from the diffraction data.

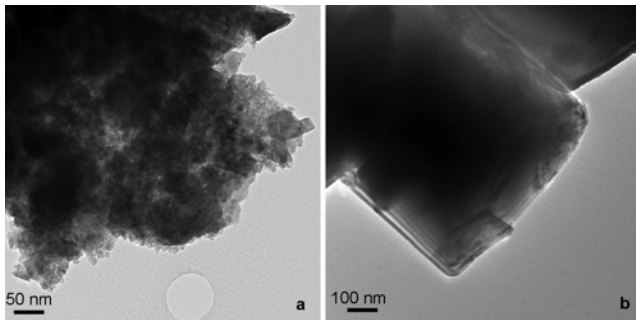


Fig 1. Franklinite (ZnFe_2O_4), Sample A (after reference⁷) a) nanocrystalline material. b) Euhedral single crystal.

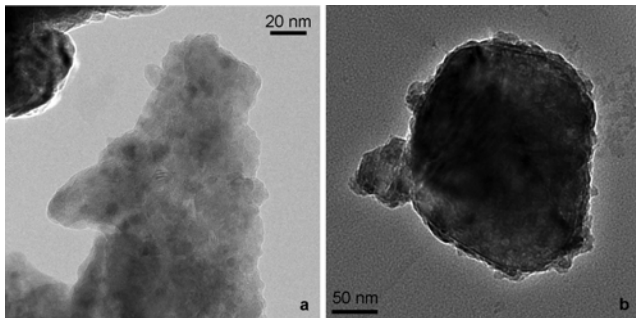


Fig 2. Iron oxides, Sample A (after reference⁷). a) Nanocrystalline mixture including hematite ($\alpha\text{-Fe}_2\text{O}_3$), goethite ($\alpha\text{-FeOOH}$), and magnetite (Fe_3O_4) or maghemite ($\gamma\text{-Fe}_2\text{O}_3$). b) Single crystal of hematite.

III.B. Sample B

Franklinite was observed as euhedral single crystals in Sample B, but not as nanocrystals. Other phases identified in Sample B included a single crystal of willemite (Zn_2SiO_4), several areas of nanocrystalline akaganéite ($\beta\text{-FeOOH}$) (Fig. 3), a particle of amorphous silica, and a single particle of phase with a Fe:Cr ratio of $\sim 4:1$ and significant concentrations of Ni and Si that could not be identified from the diffraction data.

Despite its nominal composition, akaganéite is a chloride-bearing phase,^{11,12} which probably formed after the chloride contamination was introduced into this sample. EDX spectra confirmed the presence of chlorine in the material identified as akaganéite.

III.C. Sample C

Data from 11 particles were collected from a single TEM sample from Sample C. In contrast to Samples A and B, many of the particles included more than one phase (Fig. 4), greatly complicating phase identification.

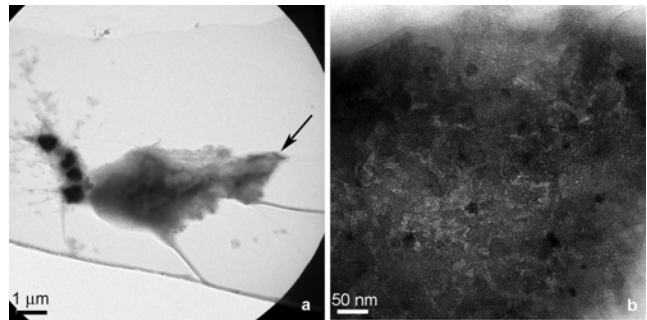


Fig 3. Akaganéite ($\beta\text{-FeOOH}$), Sample B. a) Individual particle; arrow indicates an area of akaganéite. Dark spots at left end of image are franklinite crystals. b) Higher-magnification view showing individual nanocrystals in area indicated by arrow in part a.

Fig. 4 shows two particles in which some areas (labels 6, 17, and 18) have high concentrations of Zr and others (5, 7, and 19) consist primarily of Fe. Areas 5 and 7 also contain Mn, Ni, Cu, and Zn. These compositions suggest that these particles may consist of cladding and the immediately adjacent crud layer. Unfortunately, it was not possible to identify the high-Fe phases in these particles from diffraction patterns.

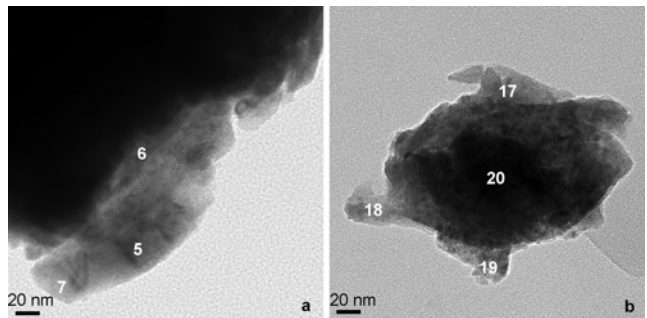


Fig. 4. Individual particles with high-Zr and high-Fe areas, Sample C.⁶ Numbers indicate locations from which EDX spectra were collected.

Figure 5 shows iron oxides from Sample C. Despite the different crystal habits, the crystals in Fig. 5a and the medium-gray area in the center of Fig. 5b are both hematite, as is the crystal labeled “36” in Fig. 5c. The EDX and diffraction data corresponding to Fig. 5a suggest that this area also contains another phase, possibly hisingerite, $\text{Fe}_2\text{Si}_2\text{O}_5(\text{OH})_4 \cdot 2\text{H}_2\text{O}$. The small, rounded domains in Fig. 5d are magnetite or maghemite.

Many of the EDX spectra from Sample C show low but significant concentrations of elements not expected in the phases identified here. In particular, many spectra from iron oxides contain detectable quantities of Na, Al, Si, and Ca. These elements suggest that small quantities of clay minerals may be present, possibly as thin coatings on the

oxides. A single particle of a high-Pb phase was also observed.

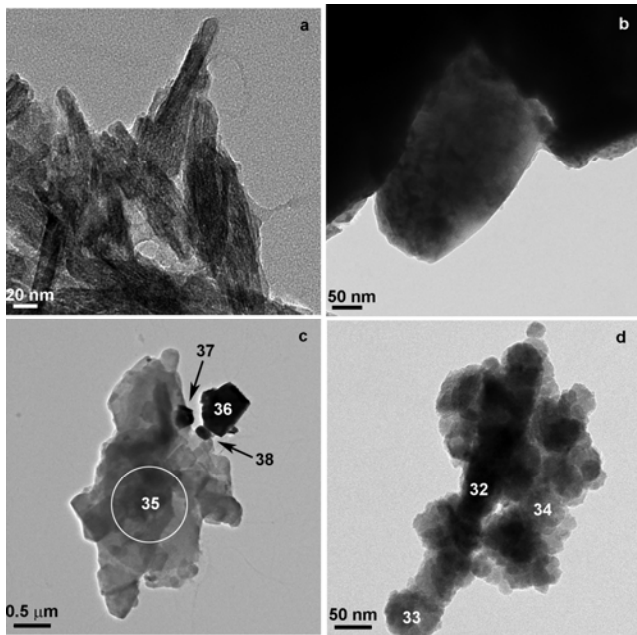


Fig. 5. Iron oxides, Sample C.⁶ Numbers indicate locations of EDX spectra. a) and b) Hematite. c) Complex particle; area of spectrum 36 is hematite; 38 is also an iron oxide, but 37 has a significant concentration of Zn and may be franklinite. The area of spectrum 35 is an unidentified aluminosilicate. d) Rounded domains of magnetite or maghemite.

III.D. Sample D

Data from eight particles and a material with poorly defined boundaries were collected from Sample D. Two of the particles were crystalline corundum ($\alpha\text{-Al}_2\text{O}_3$). These particles are assumed to be contaminants (possibly chips from the “stone” knife used to scrape the fuel rods during sample collection), and will not be described further in this paper.

Two particles from Sample D were high in Fe. The EDX spectrum from one of these particles (Fig. 6a) indicates a nearly pure iron oxide, and the diffraction data indicate that the particle is hematite. EDX spectra from the other particle (Fig. 6b) vary significantly from point to point, and contain significant concentrations of other elements (primarily Na, Al, and Si). The diffraction data from this particle contain numerous scattered reflections, which are consistent with hematite. In combination, the diffraction and EDX data suggest that the particle may contain at least four phases: an iron oxide (probably hematite), an aluminum-bearing phase, a sodium-bearing phase, and a silicate, of which only one (hematite) is well-represented in the diffraction data.

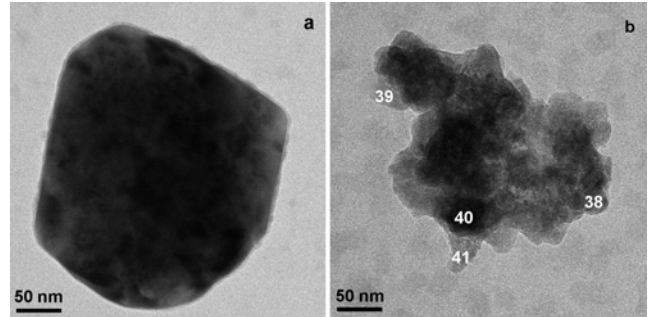


Fig. 6. High-Fe particles, Sample D.⁶ a) Euhedral crystal of hematite. b) Particle containing multiple phases, one of which is hematite.

Three of the particles from Sample D had higher concentrations of Zr than of any other element quantified. All three particles were polycrystalline, and each had a significant concentration of Fe. EDX spectra from two of the three particles also showed significant concentrations of Na, Al, and Si, and of the spectra also showed low concentrations of Ca, Na, Cu, Zn, and Sr. The high Zr concentrations suggest that these particles are fragments of cladding, possibly with small amounts of crud and aluminosilicate materials.

Two EDX spectra were collected from a high-Al, high-Si particle that became amorphous during TEM observation. One of the spectra had Al, Si, and a few atomic % of Ca, and had a Si:Al ratio of ~4:1. The other spectrum had Na and Sr in addition to the Al, Si, and Ca, and had a Si:Al ratio of ~2.5. Oxygen is qualitatively present in both spectra. Although the material in the particle could not be conclusively identified without diffraction data, it is probably clay.

One area with high-Na, high-Si material was also observed in Sample D. Boundaries of this area are sufficiently indistinct that it may not be appropriate to call it a “particle.” The EDX spectrum from this area shows ~50% Na, 30% Si, and 15% Cl, as well as lower concentrations of Al, Ca, and Sr. This spectrum is the only one from Sample D to show a significant concentration of chlorine. Oxygen is qualitatively present. It was not possible to identify the phase(s) present.

IV. DISCUSSION AND CONCLUSIONS

This paper reports identification of phases in four samples of crud from three commercially operating boiling water reactors. Phases were identified by a combination of images, energy-dispersive X-ray spectroscopy (EDX), and selected-area electron diffraction data collected using a transmission electron microscope. Samples were prepared by suspending minuscule particles in pure water, placing a drop of the water on a carbon-coated formvar substrate,

and air drying. Relative abundances of phases in the TEM samples are probably not statistically representative, and it is likely that the samples contain phases that were not observed in this study. Nonetheless, TEM offers a unique opportunity to identify the phases and observe the compositions of individual crystals. It is thus a worthwhile complement to data produced by techniques such as scanning electron microscopy and chemical analysis of dissolved samples.

One surprising result is that each of the samples contained significant quantities of materials that are probably contaminants. Samples A and B, which were collected by scraping crud from the outsides of fuel pins, contained significant quantities of chloride-bearing phases (primarily NaCl, but also KCl and akaganéite). As it is highly unlikely that significant concentrations of chlorine would be tolerated in a reactor cooling system, the chloride-bearing phases must have been somehow introduced between the time the fuel pin was removed from the reactor and the time the samples were prepared for analysis. Samples C and D (which were collected by filtering pool water) contain significant quantities of aluminosilicates (probably clays) with widely variable aluminum:silicon ratios, and Sample D contains numerous particles of corundum that may be fragments of the “stone” knife used to scrape the fuel pin during collection of the crud samples. The common presence of readily-recognized contaminants such as chlorides, clays, and alumina suggests that other phases whose compositions are more compatible with cooling-water chemistry (e.g., the crystalline silica from Sample A) may also be contaminants. If quantities of contaminants in the samples studied here are typical, the inclusion of unrecognized contaminant phases in chemical analysis data from other samples may greatly complicate attempts to interpret this data, and therefore to understand and control formation of crud.

Phases observed in sample A include franklinite, hematite, crystalline silica, a fine-grained mixture of iron oxides probably including magnetite, hematite, and goethite, an unidentified high-Ba, high-S phase, and halite (a contaminant). Phases observed in sample B included franklinite, the chloride contaminants halite and sylvite, akaganéite (indicating chloride contamination), willemite, amorphous silica, and an unidentified Fe-Cr phase. Phases identified in Sample C included hematite with a wide variation in crystal sizes and shapes, magnetite or maghemite, a high-Pb phase, and at least one kind of clay. Phases identified in Sample D included corundum (α -Al₂O₃), hematite, and an unidentified aluminosilicate that is probably a clay. High-Zr material was observed in a number of samples but not analyzed in detail because it was assumed to represent part of the cladding. EDX analyses commonly show the presence of elements not

expected from phase identifications based on diffraction data, and some diffraction patterns show “extra” reflections that would not have been produced by the identified phases. Although some of the “extra” elements may be present in solid solutions, it is likely that many of the analyses include small quantities of phases that were not identified. This is particularly true of the Na, Ca, Al, and Si in samples from Reactor C, where they may represent thin coatings of clay.

The presence of high-Zn phases (franklinite, willemite) in samples from Reactors A and B may be a consequence of Zn addition in these reactors, and the clays in samples from Reactor C may be consequences of collecting data from the reactor pool. However, these are relatively trivial conclusions, and establishing more detailed relationships between the phases observed in each sample and the chemical conditions in the reactor during formation of the crud is highly desirable. Nonetheless, the small sample volumes and numbers of particles studied and the possibility that some phases were introduced as contaminants outside the reactor make it impossible to tell whether other differences in phases observed in different samples are characteristics of the samples or artifacts of the small numbers of areas and particles examined.

Some single-crystal electron-diffraction patterns from franklinite, hematite, and willemite show kinematically forbidden reflections. Forbidden reflections in X-ray powder patterns from franklinite have been studied in detail and were determined to be from double diffraction⁸. Detailed analyses of the factors allowing the appearance of kinematically forbidden reflections can be quite complex,^{13,14} and are beyond the scope of this paper. Although the origins of the kinematically forbidden reflections in willemite and hematite are unknown, these reflections probably do not indicate significant structural differences between crystals of these phases formed inside reactors and those formed in natural environments. Thus, thermodynamic and kinetic data from naturally occurring and synthetic examples of these phases may be applicable to models of crud formation.

All of the available data indicate that crud consists of a complex, multi-phase assemblage with spatial variation on a scale so small that it must be understood using techniques such as TEM. However, the areas from which TEM data are collected are too small to identify broader patterns of compositional variation, and relative proportions of phases represented in the TEM data may not represent those in the bulk sample. Similarly, it is likely that the bulk sample contains phases not identified in the TEM data presented here. Broader patterns of chemical variation can be observed with scanning electron microscopy (SEM). Bulk chemical analyses provide relatively easy ways to observe gross changes in crud

characteristics as a result of changes in water chemistry or reactor operation, but are of limited use in identifying individual phases. Thus, crud is probably best understood by a variety of analytical techniques, each of which has its own strengths and weaknesses. TEM is clearly one such technique.

ACKNOWLEDGMENTS

The authors would like to thank Dr. Bo Cheng, the EPRI Project Manager for this study. We would also like to thank Dr. Kurt Edsinger (EPRI), Dr. Shaw Bian (Energy Northwest), and Mr. Dan Lutz (General Electric) for their assistance in obtaining and providing the samples analyzed here. Dr. Cheng, Dr. George Sabol, and Dr. Mike Pop provided helpful comments on preliminary presentations of some of this work and arranged for us to see their unpublished results on other crud samples.

The work reported here was performed in the Electron Microscopy Laboratory at the INL. The authors would like to thank EML staff members Dr. Tom O'Holleran and Mr. Mark Surchik for their assistance. Mr. Calvin D. Morgan (from the Analytical Laboratory at the INL) analyzed the chloride content of the water used for preparation of the samples from Reactors A and B. Mr. Keener Earle provided project-management services at the INL.

The work was supported by the U.S. Department of Energy, Office of Nuclear Energy, Science, and Technology, under DOE Idaho Operations Office Contract DE-AC07-05ID14517. The authors would particularly like to thank our sponsor, Tom Miller from DOE NE-30, who graciously funded this work.

REFERENCES

1. S. UCHIDA, Y. Asakura, K. Ohsumi, M. Miki, M. Aizawa, Y. Matsushima, and K. Yonezawa, "Chemical Composition of Crud Depositing on BWR Fuel Surfaces," *Journal of Nuclear Science and Technology*, **24**, 5, 385 (1987).
2. C. S. OLSEN, "The performance of defected spent LWR fuel rods in inert and dry air storage atmospheres," *Nuclear Engineering and Design*, **89**, 51 (1985).
3. T. MIZUNO, K. Wada, and T. Iwahori, "Deposition Rate of Suspended Hematite in a Boiling Water System Under BWR Conditions," *Corrosion--NACE*, **38**, 1, 15 (1982).
4. Y. NISHINO, T. Sawa, K. Ebara, and H. Itoh, "Magnetic Measurements of NiFe_2O_4 Formation from Iron Hydroxides and Oxide in High Temperature Water," *Journal of Nuclear Science and Technology*, **26**, 2, 249 (1989).
5. K. ISHIGURE, "Radiation Chemistry Related to Nuclear Power Technology," *Radiation Physics and Chemistry*, **22**, 1/2, 119 (1983).
6. D. E. JANNEY, D. L. Porter, O. K. Earle, R. Demmer, J. J. Giglio, M. W. Huntley, M. G. Jones, and J. L. Peterson, "Report to the DOE on the Crud II Project," Report No. INL/EXT-06-11742, 2006.
7. D. E. JANNEY, D. L. Porter, and J. L. Peterson, "Characterization of Phases in "Crud" from Boiling Water Reactors by Transmission Electron Microscopy," *Journal of Nuclear Materials*, **362**, 104 (2007).
8. S. LUCCHESI, U. Russo, and A. Della Giusta, "Cation distribution in natural Zn-spinels: franklinite," *European Journal of Mineralogy*, **11**, 501 (1999).
9. R. J. HILL, J. R. Craig, and G. V. Gibbs, "Systematics of the spinel structure type," *Physics and Chemistry of Minerals*, **4**, 317 (1979).
10. G. A. WAYCHUNAS, "Crystal Chemistry of Oxides and Oxyhydroxides," in *Oxide Minerals: Petrologic and Magnetic Significance*, edited by D.H. Lindsley, *Reviews in Mineralogy*, **25** (Mineralogical Society of America, Washington, D.C.), 11 (1992).
11. J. E. POST and V. F. Buchwald, "Crystal structure refinement of akaganéite," *American Mineralogist*, **76**, 272 (1991).
12. J. E. POST, P. E. Heaney, R. B. Von Dreele, And J. C. Hanson, "Neutron and temperature resolved synchrotron X-ray powder diffraction study of akaganéite," *American Mineralogist*, **88**, 782 (2003).
13. P. HIRSCH, A. Howie, R. Nicholson, D. W. Pashley, and M. J. Whelan, *Electron Microscopy of Thin Crystals*, ed., Krieger Publishing Company, Malabar, FL (1977).
14. D. B. WILLIAMS and C. B. Carter, *Transmission Electron Microscopy*, ed., Plenum, New York (1996).